

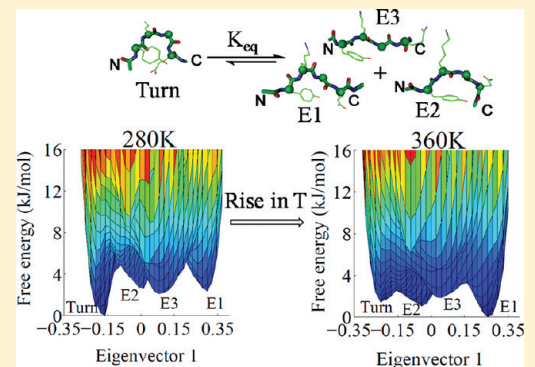
For the Sequence YKGQ, the Turn and Extended Conformational Forms Are Separated by Small Barriers and the Turn Propensity Persists Even at High Temperatures: Implications for Protein Folding

Harpreet Kaur and Yellamraju U. Sasidhar*

Department of Chemistry, Indian Institute of Technology Bombay, Powai, Mumbai 400 076, India

Supporting Information

ABSTRACT: The folding of the sequence $^{21}\text{DTVKLMLYKGQPMTFR}^{35}$ from staphylococcal nuclease into a β -hairpin, nucleated by the turn region YKGQP, is known to be an early folding event. With YKGQ being the shortest sequence for a β -turn model and in view of its importance to the folding of staphylococcal nuclease, we investigated the thermodynamics of turn formation at a range of temperatures from 280 to 380 K, with a regular interval of 10 K. Eleven independent molecular dynamics simulations (under NPT conditions) were performed using the GROMACS package of programs and the OPLS-AA/L all-atom force field, each for a time period of 1 μs . Turn formation is supported by enthalpy at lower temperatures, while entropy supports it at higher temperatures. There are modest free energy barriers between turn and extended conformational ensembles. The turn propensity persists even at elevated temperatures. The role of proline in driving the turn formation has been re-examined, and it is inferred that the absence of proline does not affect turn propensity.



1. INTRODUCTION

In the crystal structure of staphylococcal nuclease (1SNC),¹ two antiparallel strands 2 and 3 of a β -hairpin are connected by a sequence YKGQ that adopts a type I' β -turn conformation. Previous hydrogen–deuterium exchange studies suggest that the region corresponding to the β -hairpin ($^{21}\text{DTVKLMLYKGQPMTFR}^{35}$) formed by strands 2 and 3 forms early during refolding of staphylococcal nuclease.^{2,3} Further, molecular dynamics (MD) simulation study on the hairpin peptide revealed that the sequence $^{27}\text{YKGQP}^{31}$ initiates the folding process and it adopts a type II β -turn conformation.⁴ Side-chain association of Y and P residues was observed to mark an important event in nucleating the hairpin folding. This was supported by another MD study on the peptide sequence $^{27}\text{YKGQP}^{31}$, where a type II β -turn possessing Y–P side-chain association was found to characterize a deep minimum in the free energy landscape, thus implicating the importance of the β -turn formed by sequence YKGQ.⁵ Further on reanalyzing the trajectories for folding of the hairpin peptide, it was observed that the peptide sequence YKGQ undergoes a transition from a type II to type I' turn conformation during its folding process.

β -turns can activate protein folding by acting as initiation sites, as they bring together relatively distant regions of the poly-peptide chain to promote further folding events.^{6–8} Since YKGQ is strongly implicated to have played a role in folding of staphylococcal nuclease, by initiating hairpin formation in the protein, it is a candidate for characterizing structural and dynamical features of an active β -turn. Deciphering the

enthalpic and entropic contributions to turn formation in a short tetra-peptide YKGQ would provide a conducive approach to further understand the principles governing initial events in protein folding. Though the thermodynamics of α -helix or β -sheet formation in small peptides has been analyzed in many studies,^{9–12} to our knowledge, only a handful of studies have been done so far addressing particularly the thermodynamics of much shorter β -turn forming segments.^{13,14}

In this study, we investigated the thermodynamics of β -turn formation in the sequence YKGQ. We performed 11 MD simulations at 11 temperatures starting from an unfolded conformation of the peptide. Moreover, here the proline residue has been removed from the peptide sequence, thus withdrawing an important hydrophobic association with the tyrosine residue. Hence, in this study, we tried to re-examine whether indeed such an interaction is important for turn formation in the peptide sequence YKGQ. It was observed that, regardless of the absent Y–P side-chain association, YKGQ still undergoes turn formation, even at elevated temperatures. Investigation of the role played by various thermodynamic parameters, such as folding free energy, folding enthalpy, and folding entropy of turn formation, has been analyzed and their temperature dependence has also been discussed.

Received: October 25, 2011

Revised: March 1, 2012

Published: March 3, 2012

2. METHODS

2.1. System for Simulation. The coordinates of the sequence YKGQ were taken from the crystal structure of staphylococcal nuclease¹ with the ends protected by an acetyl group ($-\text{CH}_3\text{CO}$) group at the N-terminus and N-methyl ($-\text{NHCH}_3$) group at the C-terminus. Thus, the sequence of the peptide used for simulation was Ac1-Y2-K3-G4-Q5-NMe6. The polyproline II (PPII) conformation ($\Phi = -76^\circ$ and $\Psi = 149^\circ$), to model the unfolded state,^{15–19} of the peptide was derived from the conformation of the peptide from the crystal structure of staphylococcal nuclease (1SNC) using DeepView (<http://www.expasy.org/spdbv/>). The peptide was placed in a cubic box of edge length 3.46 nm, and periodic boundary conditions were used. The box was solvated with 3975 SPC water molecules.²⁰ The total charge on the peptide was +1 and was neutralized by replacing one water molecule with a Cl^- ion.

2.2. Molecular Dynamics. The thermodynamics of the turn formation of YKGQ was studied at a series of 11 different temperatures ranging from 280 to 380 K at an interval of 10 K (i.e., at 280, 290, 300, 310, 320, 330, 340, 350, 360, 370, and 380 K). Eleven MD simulations were performed using the GROMACS package of programs,²¹ version 4.0.4, with the OPLS-AA/L all-atom force field²² on Intel Xeon quad core processor based machines running CentOS 4.3 (www.centos.org). The total simulation length for each of the simulations was 1 μs . A short (80 ns) unfolding simulation of the complete protein sequence, starting from the crystal structure of staphylococcal nuclease,¹ at 500 K was also performed.

The electrostatic interactions were treated by the particle mesh Ewald (PME) method,^{23,24} with a Coulomb cut off of 1 nm, a Fourier spacing of 0.12 nm, and an interpolation order of 4. The van der Waals interactions were treated using the Lennard-Jones potential and a switching function with a cutoff distance of 1 nm and a switching distance of 0.9 nm. For energy minimization, the steepest descent algorithm was used with a tolerance of 100 $\text{kJ mol}^{-1} \text{nm}^{-1}$ and convergence was obtained. After energy minimization, position restrained MD (keeping the peptide atoms restrained to fixed positions) was carried out for 50 ps for all 11 systems at their respective reference temperatures. This step distributes the water molecules homogeneously around the peptide, removing any voids present. Initial velocities required to start the simulation were drawn from the Maxwell velocity distribution at respective simulation temperature. Final productive MD was then performed with an integration time step of 2 fs. To constrain the bonds, the LINCS algorithm was used.²⁵ Coordinates were saved after every 0.5 ps, and velocities were saved after every 20 ps. Temperature and pressure coupling were done for both peptide and solvent separately using the Berendsen method.²⁶ Respective simulation temperatures were used as reference temperatures with a time constant of 0.1 ps, and reference pressure was kept as 1 bar with a time constant of 1 ps.

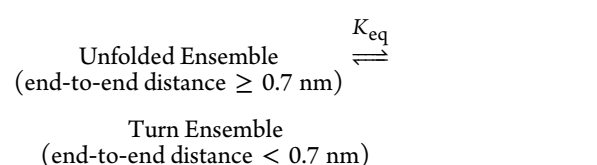
2.3. Analysis of Molecular Dynamics Trajectories. Analyses of the obtained trajectories were carried out using analysis tools provided by the GROMACS package. For secondary structure assignment, the DSSP program²⁷ was used as implemented in GROMACS. To cluster the conformations sampled, an algorithm described by Daura et al.²⁸ was used, as implemented in GROMACS with a cutoff of 0.1 nm. The distance between Y2 and Q5 side-chains was evaluated by calculating the distance between the respective centers of mass of the side-chains of the two residues. For

formation of a hydrogen bond, a cutoff distance of 0.26 nm, which is the sum of the van der Waals radii of hydrogen (0.12 nm) and acceptor (oxygen = 0.14 nm), and an acceptor–donor–hydrogen angle of 30° were considered. Peptide–water interactions were investigated by calculating the radial distribution functions (RDFs) of water oxygen around peptide backbone amide hydrogen ($g_{\text{NH}-\text{Ow}}$) and water hydrogens around peptide backbone carbonyl oxygen ($g_{\text{CO}-\text{Hw}}$), by using the g_rdf program incorporated in GROMACS. To analyze the water network around peptide atoms, arrangement of water molecules within a distance of 0.35 nm, corresponding to the approximate radius of the first solvation shell of water inferred from RDF plots, from the peptide atoms was considered. Representative structures from turn and unfolded conformational ensembles, observed at 280 and 360 K, were chosen on the basis of cluster analysis (central structures of top two clusters). The network of water molecules forming hydrogen bonded bridges between different parts of the peptide chain in each representative structure was examined, using VMD.²⁹

All figures were generated using Matlab, VMD, and Xmgrace (<http://plasma-gate.weizmann.ac.il/Grace>). Matlab (<http://www.math-worls.com>) software was also used for analysis. We have presented the results mainly for a lower temperature simulation (at 280 K) and a higher temperature simulation (at 360 K). Results obtained at other temperatures have been presented in Figures S1–S11 and Table S1 of the Supporting Information.

2.4. Thermodynamics of β -Turn Formation. In 1973, Lewis et al. analyzed 135 bends found in crystal structures of eight proteins and observed characteristic distances between C^α of its first and fourth residues ($R_{i,i+3}$) corresponding to different structures present in proteins such as α -helix, extended, and bend conformations.³⁰ They found that the distance $R_{i,i+3}$ acts as a boundary between folded and extended structures. On the basis of this, a four residue turn can be considered to be present if the distance between C^α atoms of its first and fourth residues is less than 0.7 nm. This distance is referred to as the end-to-end distance in this paper. Further, turns can be both closed (with a $4 \rightarrow 1$ hydrogen bond) and open (without a $4 \rightarrow 1$ hydrogen bond). Turns can also be characterized by the dihedral angles adopted by the corner residues (second and third residues) in a four-residue turn.^{30–36}

On the basis of the above convention, we consider that a turn is present if the end-to-end distance (between C^α atoms of Y2 and Q5) is <0.7 nm. We further note that the analysis of the free energy landscape (see section 3.6) of the peptide shows that the turn conformers, sampling the free energy minimum corresponding to turn ensemble, have an end-to-end distance <0.7 nm. Thus, in order to analyze the thermodynamics of turn formation, we assume a two-state model as follows:



where K_{eq} is the equilibrium constant of the reaction and is expressed as

$$K_{\text{eq}} = \frac{\text{Fraction folded}}{\text{Fraction unfolded}} \quad (1)$$

We considered fraction folded as the fraction of population possessing end-to-end distance ($C_{Y_2}^\alpha - C_{Q_5}^\alpha$ distance) <0.7 nm and more extended conformations (having end-to-end distance ≥ 0.7 nm) as fraction unfolded. To ensure adequate sampling of all conformations, we have plotted fraction folded with respect to the simulation time (Figure S1 of the Supporting Information). We found that the folding of peptide YKGQ reached equilibrium in all the cases after 1 μ s of simulation time. Also, the simulations at higher temperatures attained convergence earlier than those at lower temperatures. The free energy change ($\Delta G_{U \rightarrow F}$) for folding of the β -turn can be calculated by using the following equation:

$$\Delta G_{U \rightarrow F} = -RT \ln K_{eq} \quad (2)$$

where R is the gas constant. For $\Delta G_{U \rightarrow F}$ vs temperature data, the method of least-squares was used for curve fitting, as implemented in MATLAB. Linear, quadratic (parabolic), and cubic curves were tried to fit and compared, resulting in a badly conditioned polynomial for the cubic curve. The linear fit gave a residual sum of squares as 0.70, while the quadratic fit gave a value of 0.45, suggesting a better fit for later. Further linear fit gave an R^2 value of 0.8 in comparison to a better R^2 value of 0.9 for quadratic fit. Hence, the quadratic fit is used to deduce thermodynamic quantities.

Thermodynamic quantities like change in folding entropy ($\Delta S_{U \rightarrow F}$) and change in folding enthalpy ($\Delta H_{U \rightarrow F}$) can be derived from the fitted parabolic curve to $\Delta G_{U \rightarrow F}$ vs temperature data, using the following equations:

$$\Delta G_{U \rightarrow F} = \Delta H_{U \rightarrow F} - T\Delta S_{U \rightarrow F} = aT^2 + bT + c \quad (3)$$

$$\Delta S_{U \rightarrow F} = -\partial(\Delta G_{U \rightarrow F})/\partial T = -(2aT + b) \quad (4)$$

$$\Delta H_{U \rightarrow F} = \Delta G_{U \rightarrow F} + T\Delta S_{U \rightarrow F} = -aT^2 + c \quad (5)$$

where $a = -1.6 \times 10^{-4}$ kJ mol $^{-1}$ K $^{-2}$, $b = 0.12$ kJ mol $^{-1}$ K $^{-1}$, and $c = -20.8$ kJ mol $^{-1}$.

2.5. Essential Dynamics Analysis. Principal components of the C^α atomic displacement vector responsible for the conformational changes observed in the peptide were analyzed using essential dynamics analysis methods described by Amadei et al.³⁷ and de Groot et al.³⁸ A covariance matrix of positional fluctuations of C^α atoms was constructed and diagonalized to obtain eigenvalues and eigenvectors. The eigenvalues were ordered in the descending order of their magnitude. The first and second eigenvectors with highest and second highest eigenvalues accounted for more than 80% of the overall positional fluctuations in YKGQ at all temperatures. Thus, the essential plane was defined by the first two eigenvectors and the free energy landscape was constructed in the same plane.

2.6. Free Energy Calculation from Essential Dynamics Analysis. The essential plane constructed from the two most relevant eigenvectors was divided into 30×30 grid cells giving a total of 900 cells. Conformations sampled at every 0.5 ps were projected on this plane, and the number of points obtained in each cell was counted. At equilibrium, the number of points obtained in each grid cell corresponds to the probability of the conformations sampled by the grid cells. The grid cell containing the maximum number of points is then assigned as the reference cell, as described by Daidone et al.,¹⁰ with a free energy value of zero being assigned to it. Free energies are

then assigned to all the other cells with respect to this reference cell. For the i th cell, this can be mathematically expressed as

$$\Delta G_{ref \rightarrow i} = -RT \ln N_i/N_{ref} \quad (7)$$

where N_i and N_{ref} are the number of points in the i th and reference cell, respectively, R is the gas constant, and T is the temperature corresponding to each simulation set.

3. RESULTS

3.1. The Peptide YKGQ Samples Compact and Extended Conformations during the Simulations, Compact (Turn-Like) Conformations Being More Stable at Lower Temperatures. To measure the extent of compactness of the peptide, we calculated the radius of gyration (R_g) of the backbone atoms and end-to-end ($C_{Y_2}^\alpha - C_{Q_5}^\alpha$) distance distribution at all temperatures. It can be seen that both compact and extended (unfolded) conformations were observed (Figure 1). As the temperature increases, the

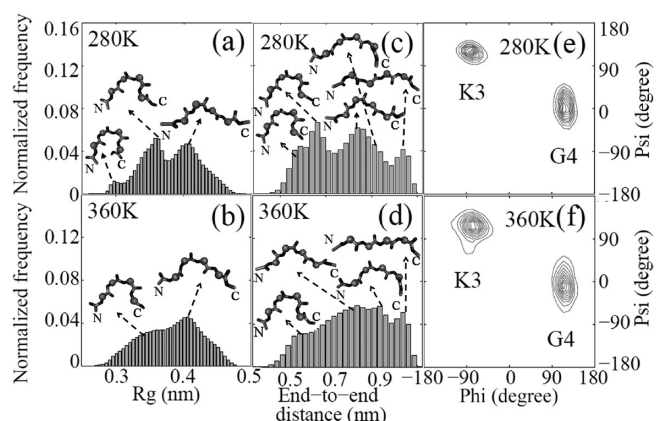


Figure 1. Frequency distribution of radius of gyration (R_g) of peptide backbone (left panels), end-to-end distance (middle panels), and probability contour plots (right panels, top 10 contours are shown exclusively for the turn ensemble) for backbone dihedral angles of corner residues, K3 and G4, at 280 K (a, c, e) and 360 K (b, d, f) of the YKGQ peptide. Greater sampling of type II β -turn-like conformations^{30,36} (end-to-end distance <0.7 nm and approximate backbone dihedral angles: K3 Phi = -60° , K3 Psi = 120° , G4 Phi = 80° , G4 Psi = 0° , with a standard deviation of about $\pm 30^\circ$) was observed at lower temperatures in comparison to higher temperatures.

height of the peaks corresponding to compact (turn-like) structures, with lower R_g (Figure 1a and b and Figure S2 of the Supporting Information) and end-to-end distance <0.7 nm (Figure 1c and d and Figures S3 and S4 of the Supporting Information), decreases, indicating greater sampling of compact structures at lower temperatures. Analysis of backbone dihedral angles of corner residues, K3 and G4, for the frames corresponding to the turn ensemble indicate formation of type II like β -turn conformation³⁶ at all of the temperatures (Figure 1e and f and Figure S5 of the Supporting Information).

Construction of free energy landscapes in the essential plane (as described in Methods) displayed four conformational minima at all temperatures (Figure 2a and Figure S6 of the Supporting Information). We mapped the frames possessing end-to-end distance <0.7 nm on the essential plane (Figure 2b) for the 280 K simulation. Analysis of the structures corresponding to each minimum in the corresponding free energy landscape (detailed analysis presented later in section 3.6) revealed that the probability contour plots for frames

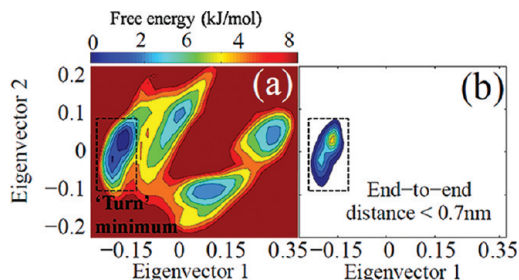


Figure 2. Comparison of (a) free energy landscape and (b) probability contour plot for frames possessing end-to-end distance < 0.7 nm in the entire trajectory at 280 K, mapped on the essential plane. Correspondence between the turn ensemble characterized by an end-to-end distance < 0.7 nm, and the observed “Turn” minimum in the free energy landscape at 280 K can be seen. In (b), relatively higher frequency contours are represented by yellow color, while lower frequency contours are represented by blue color.

possessing end-to-end distance < 0.7 nm occupied the same region, with respect to eigenvectors 1 and 2, as that of the “Turn” minimum (compare Figure 2a and b). Thus, the free energy landscape of the peptide YKGQ corroborates a two-state model, where conformations possessing end-to-end distance < 0.7 nm represent the folded ensemble and those with an end-to-end distance ≥ 0.7 nm constitute the unfolded ensemble, used in thermodynamics analysis.

Further, variation of secondary structure as a function of time monitored by the DSSP program²⁷ (Figure 3) showed rapid switching between the two (turn and coil) conformational ensembles with a rise in temperature.

3.2. A Nonlinear Relationship between the Folding Free Energy Change and Temperature Is Observed. Folding free energy change ($\Delta G_{U \rightarrow F}$) was calculated as mentioned in Methods for each temperature (Figure 4a). A nonlinear relationship between $\Delta G_{U \rightarrow F}$ and temperature implied that the folding entropy change ($\Delta S_{U \rightarrow F}$) and folding enthalpy change ($\Delta H_{U \rightarrow F}$) are temperature dependent. Figure 4 shows the variation of various thermodynamic parameters with temperature, and their values are listed in Table S1 of the Supporting Information. A positive $\Delta G_{U \rightarrow F}$ value (Figure 4a) implies that the equilibrium between extended and turn conformational ensembles favors extended (or unfolded) conformation over the turn conformation at all temperatures. As the temperature increases, the $\Delta G_{U \rightarrow F}$ values become more positive and therefore turn forming propensity further decreases. It can be seen that the turn formation in YKGQ is enthalpy driven at lower temperatures (Figure 4b) and at high temperatures entropy (Figure 4c) relatively stabilizes the turn conformation.

3.3. Intrapptide Hydrogen Bonds Promote Marginal Stability of Turn Conformation in YKGQ at All Temperatures. We analyzed the specific hydrogen bond interactions that participated in stabilizing turn conformation. Calculation of the percentage of hydrogen bonds observed in YKGQ, before and after turn formation at each temperature, revealed that only two hydrogen bonds persist for more than 1% of the time in the turn ensemble—one between peptide backbone atoms, Q5NH:Y2CO, and another between Y2 backbone and Q5 side-chain, Y2NH:Q5OE1 (Figure 5). These hydrogen bonds facilitate turn formation in YKGQ. Moreover, analysis of simultaneous occurrence of Q5NH:Y2CO and Y2NH:Q5OE1 hydrogen bonds showed zero correlation coefficient. Therefore,

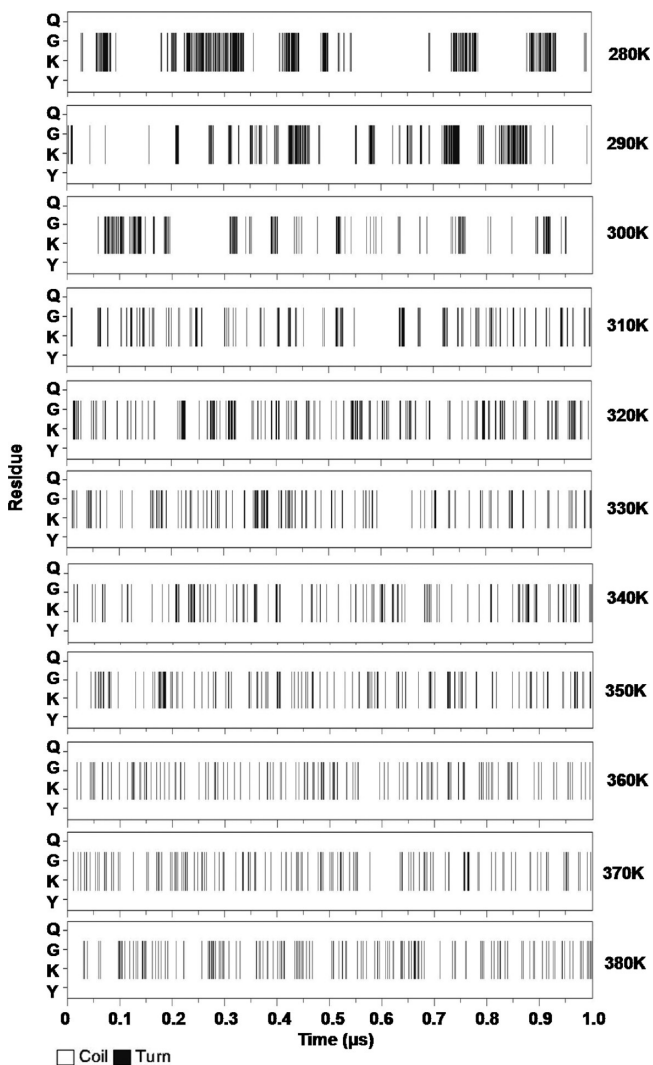


Figure 3. Variation of secondary structure of YKGQ peptide as a function of time, determined by the program DSSP.²⁷ Rapid switching between turn and coil (extended) conformations was observed with a rise in temperature.

these bonds are formed exclusively one at a time in the turn ensemble and they interchangeably take part in stabilizing the turn conformation. Also, the Q5NH:Y2CO bond leads to formation of a tighter turn in comparison to turn conformation adopted due to formation of a Y2NH:Q5OE1 bond (compare the end-to-end distances in Figure 5b and c). Also, with rise in temperature, the percentage of hydrogen bonds formed decreases in correspondence to the observed lower propensity of turn formation at higher temperatures (Figure 5a). An abrupt decrease in Y2NH:Q5OE1 hydrogen bond was observed upon a rise in temperature, relative to the decrease seen for the Q5NH:Y2CO hydrogen bond.

3.4. Y2–Q5 Side-Chain Association Stabilizes Turn Conformation. Studies on side-chain packing interactions suggest that, if the minimum distance between the side-chain atoms is ≤ 0.55 nm, then a contact between two side-chains can be considered significant.³⁹ Considering this distance as the cutoff for observing packing interaction between the two side-chains, it was observed that Y2 and Q5 side-chains do interact with each other in order to promote turn formation (Figure 6 and Figure S7 of the Supporting Information). It was also

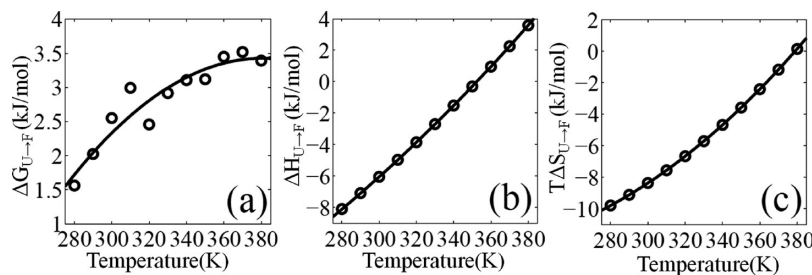


Figure 4. Temperature variation of thermodynamic functions (a) $\Delta G_{U \rightarrow F}$, (b) $\Delta H_{U \rightarrow F}$, and (c) $T\Delta S_{U \rightarrow F}$ for turn formation in the peptide YKGQ, based on the two-state model. In (a), a least-squares fit curve is shown (solid line) along with data points (circles). In (b) and (c), $\Delta H_{U \rightarrow F}$ and $T\Delta S_{U \rightarrow F}$ are derived from the least-squares fit curve.

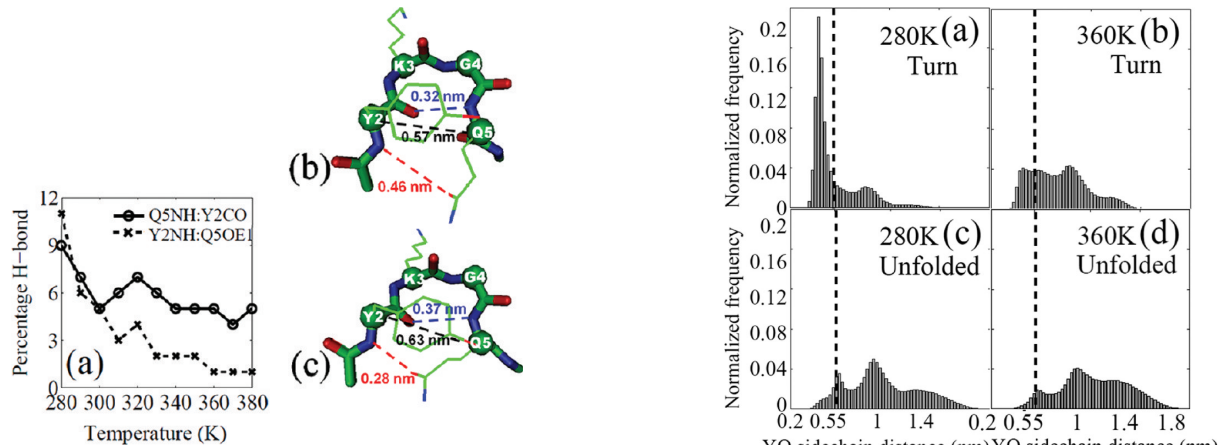


Figure 5. (a) Percentage sampling of the two significant hydrogen bonds (Q5NH:Y2CO and Y2NH:Q5OE1) in turn ensemble at each temperature. Structures of conformations possessing (b) Q5NH:Y2CO and (c) Y2NH:Q5OE1 hydrogen bonds at 280 K are shown. These hydrogen bonds form exclusive of each other. It can be seen that the Q5NH:Y2CO bond leads to formation of a tighter turn (see the end-to-end distance shown in black). Central structures from the most populated cluster derived from the turn ensemble at 280 K possessing either of the two hydrogen bonds, respectively, are shown. Note that the two turn conformations shown here are type II like. Color code for measured distances: black – end-to-end distance, red – between amide nitrogen of Y2 and side chain oxygen of Q5, blue – between amide nitrogen of Q5 and carbonyl oxygen of Y2.

observed that the Y–Q side-chain association in the turn ensemble is more stable at lower temperatures (Figure 7a). Structures representing Y–Q side-chain association in the turn conformation sampled at 280 K are shown in Figure 7b and c. Moreover, in corroboration with this, calculation of solvent accessible surface area (SASA) of the unfolded and turn conformational ensemble showed that both Y2 and Q5 undergo a relative burial upon turn formation. Further analysis of change in average values for SASA upon folding showed that the two residues are more buried at lower temperatures (Figure 8 and Figure S8 of the Supporting Information), thus implicating the role played by Y–Q side-chain association in turn formation.

3.5. Role of Solvent in Turn Formation in YKGQ. Radial distribution functions (RDF) of water hydrogen atoms around carbonyl oxygen (g_{CO-H_w}) for the YKGQ peptide displayed a sharp peak at a distance of ~ 0.2 nm, for all four residues (Figure 9a and b and Figure S9 of the Supporting Information). Similarly, a peak was observed at ~ 0.2 nm in the RDF plots for water oxygen atoms around backbone amide hydrogen (g_{NH-Ow}), for all four residues (Figure 9c–f and Figure S9 of the Supporting Information).

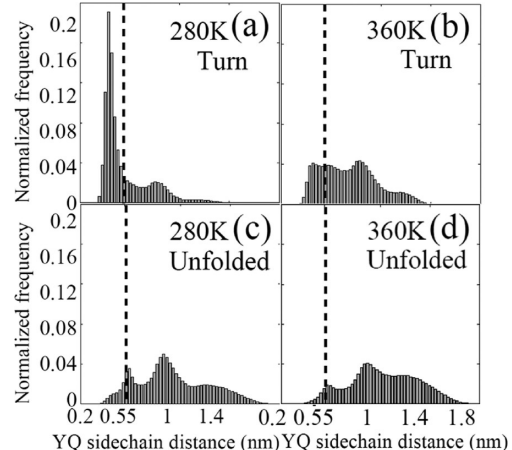


Figure 6. Comparison of Y2–Q5 side-chain distance distribution in turn (a, b) and unfolded ensembles (c, d) at 280 K (left panels) and 360 K (right panels). Y2 and Q5 side-chains are considered to be interacting if the Y2–Q5 side-chain distance is ≤ 0.55 nm (marked by broken line).³⁹ Y–Q side chain association appears to stabilize turn conformation in YKGQ.

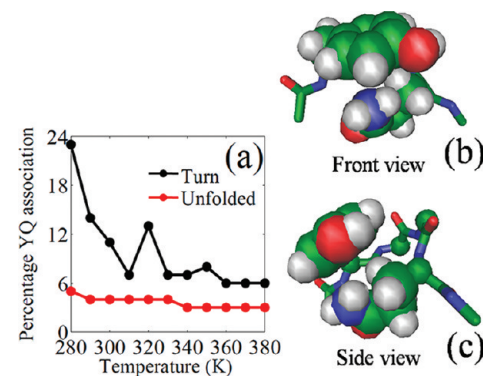


Figure 7. (a) Percentage sampling of Y–Q side-chain association ($Y2-Q5$ side chain distance ≤ 0.55 nm) in turn and unfolded ensemble in YKGQ at each temperature. Y–Q side chain interaction weakens as the temperature increases. Central structures, representing Y–Q association, from the most populated cluster derived from the turn ensemble at 280 K (b, c) are shown.

the Supporting Information). The observed peak at 0.2 nm indicates the presence of a hydrogen bond. Such an interpretation is supported by the literature.^{40–42} Comparison of RDFs for folded and unfolded conformational ensembles showed that the observed maximum at 0.2 nm displayed a relatively stronger (larger) peak for unfolded ensembles for Y2NH, Y2CO, and Q5NH (Figure 9), indicating greater

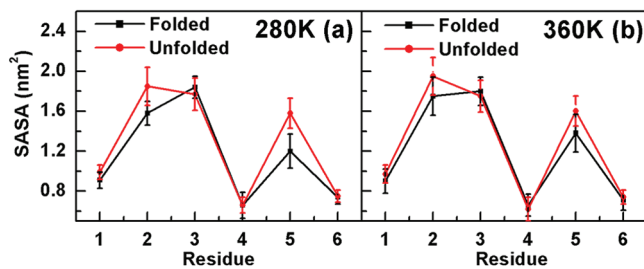


Figure 8. Solvent accessible surface area (SASA) of each residue in turn and unfolded conformational ensembles at (a) 280 K and (b) 360 K for the Ac1-Y2-K3-G4-Q5-NMe6 sequence of the peptide. Y2 and Q5 undergo a relative burial upon turn formation. Average change in SASA upon turn formation was observed to be relatively larger at lower temperatures (280 K), correlating with stronger Y–Q side chain association at lower temperatures (see also Figure 6a). K3 remains solvent exposed at all temperatures, irrespective of the conformation sampled by the peptide. The standard deviations in observed SASA are shown as error bars.

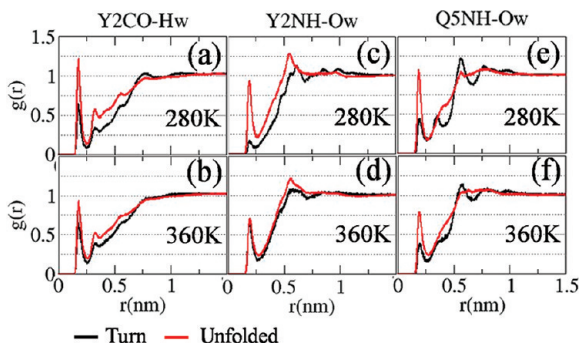


Figure 9. Radial distribution function (RDF) of the water atoms around YKGQ peptide backbone atoms. RDF of water hydrogen atoms around backbone carbonyl oxygen ($g_{\text{CO}-\text{H}_w}$) for Y2 (left panels), water oxygen atoms around backbone amide hydrogen ($g_{\text{NH}-\text{O}_w}$) for Y2 (middle panels) and Q5 (right panels) at 280 K (a, c, e) and 360 K (b, d, f), respectively, for the peptide YKGQ.

solvation of these atoms in the unfolded conformation. As described earlier in section 3.3, these atoms (i.e., Y2NH, Y2CO, and Q5NH) are involved in intrapeptide hydrogen bonding—Q5NH:Y2CO and Y2NH:Q5OE1—in the turn conformation. Therefore, these atoms are less available for hydrogen bonding with solvent atoms, thereby resulting in a weaker peak in the corresponding RDF plot for the turn ensemble. All other residues displayed little or no difference in the NH–O_w and CO–H_w RDF plots for the turn and unfolded conformational ensembles (Figure S9 of the Supporting Information). As reported earlier (section 3.3), with a rise in temperature, the percentage sampling of these intrapeptide hydrogen bonds decreases. It was observed that, for Y2, with a rise in temperature, the $g_{\text{NH}-\text{O}_w}$ peak height (at 0.2 nm) for the turn conformational ensemble increases substantially. This correlates with the lesser sampling of the Y2NH:Q5OE1 hydrogen bond at higher temperatures (~11% at 280 K and ~1% at 360 K, in the respective turn conformational ensembles). However, no major change in peak heights was observed in the case of $g_{\text{CO}-\text{H}_w}$ plots for Y2 and Q5 upon a rise in temperature. This may be attributed to a smaller change observed in Q5NH:Y2CO hydrogen bond sampling upon a rise in temperature (~9% at 280 K and ~5% at 360 K, in the respective turn conformational ensembles).

We also analyzed the arrangement of water molecules in both turn and unfolded conformational ensembles (see Methods, section 2.3) at 280 and 360 K. A relatively greater number of water molecules forming bridges (stronger network of hydrogen bonded water molecules) connecting different parts of the peptide was observed, at lower temperatures (Figure 10).

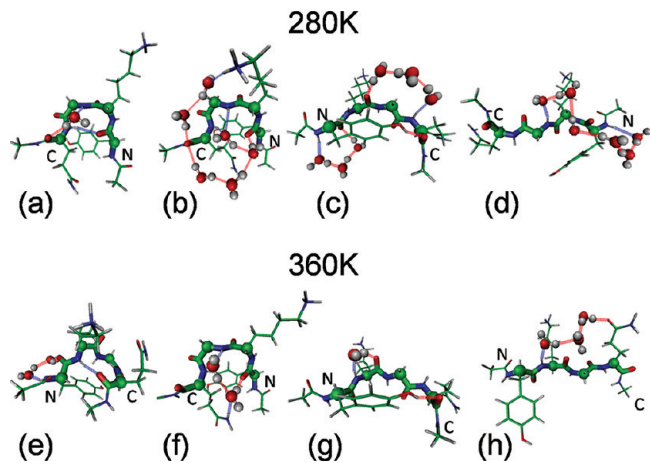


Figure 10. Network of bridging water molecules connecting different parts of the YKGQ peptide chain. Central structures from the top two clusters of the turn conformational ensemble (a and b at 280 K and e and f at 360 K) and unfolded conformational ensemble (c and d at 280 K and g and h at 360 K) are shown. A relatively greater number of water molecules forming bridges were observed at lower temperatures, for both turn and unfolded structures. Water bridges stabilizing turn conformations by connecting end residues of the peptide chain were observed for turn structures, while nearby residues were connected by water bridges in the case of unfolded structures. Water bridges stabilize open β -turns (b), while intramolecular hydrogen bonds stabilize closed β -turns (a).

On comparing water bridges observed in turn and unfolded structures (consider structures for 280 K simulation, Figure 10a–d), it can be seen that the water bridges bring the two opposite ends of the peptide chain close to each other in the turn ensemble, while, in the case of unfolded structures, bridges were observed between adjacent residues. Apart from this, considering the turn ensemble at 280 K, in the case of the structure possessing a closed β -turn (with a 4 → 1 hydrogen bond, Figure 10a), a single water molecule bridges the nearby residues of the peptide chain. However, in the case of an open β -turn (without a 4 → 1 hydrogen bond, Figure 10b), a bigger network of water molecules connects the two ends of the peptide chain. Thus, water bridges (forming peptide–water–peptide hydrogen bonds) stabilize open β -turns, while intramolecular hydrogen bonds stabilize closed β -turns. There are observations in the literature to this effect.^{43,44} Thus, water is seen to play an important role in the folding/unfolding dynamics of the β -turn in YKGQ.

3.6. Free-Energy Landscapes Reveal a Temperature Dependent Conformational Transition between Two of the Four Conformational Free Energy Minima Observed in the Essential Plane. Structures corresponding to the most populated cluster for the “Turn” conformation and each of the three extended conformations described as “E1”, “E2”, and “E3” (based on an increasing order of end-to-end distance) are shown for 280 and 360 K simulation in Figure 11. These minima occupy similar positions at all the temperatures, and a given minimum samples similar conformations at all of the

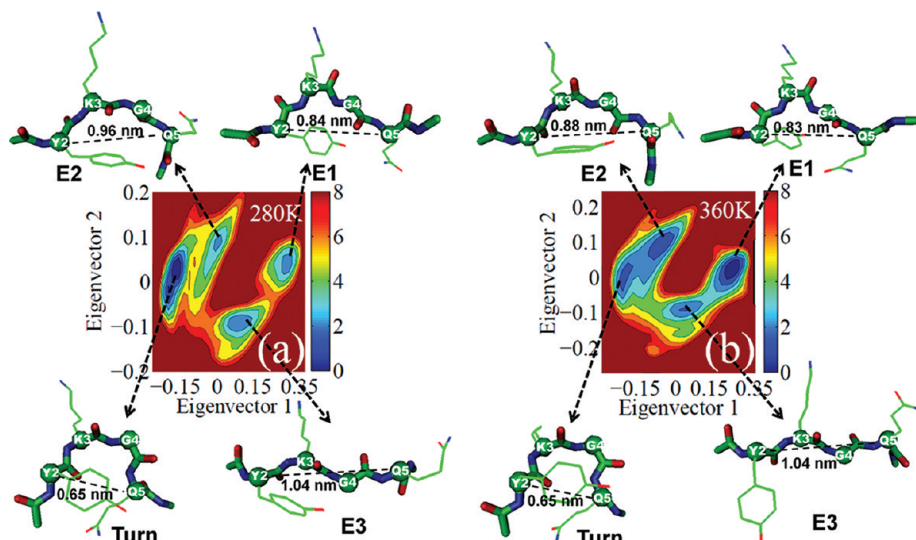


Figure 11. Free energy (in kJ/mol) landscape of the peptide YKGQ at (a) 280 K and (b) 360 K, with the structures corresponding to each minimum. “Turn”, “E1”, “E2”, and “E3” represent turn-like and three types of extended (or unfolded) conformations in increasing order of their end-to-end distance (shown in the figure). Similar conformations of the peptide backbone were observed for corresponding Turn, E1, E2, and E3 structures at each temperature. Also, for each of the different temperatures, all four structures sample a similar region of the corresponding free energy landscape, with respect to eigenvectors 1 and 2. Note that each minimum broadens with a rise in temperature, implying an increase in conformational entropy at higher temperatures.

temperatures. At lower temperatures (280–300 K), the turn conformation was observed to be having the lowest free energy, whereas, at higher temperatures (330–380 K), the extended conformation corresponds to the lowest free energy minimum (Figure 12 and Figure S10 of the Supporting Information).

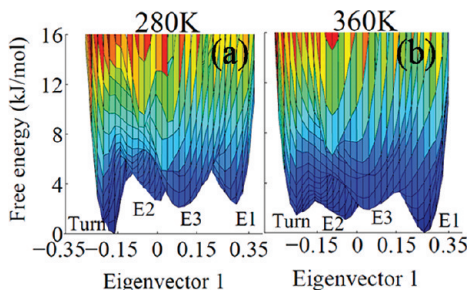


Figure 12. Projection of the free energy surface on eigenvector 1 at (a) 280 K and (b) 360 K. Comparison of the free energy of turn and extended conformations at different temperatures showed a switching behavior. At lower temperatures (280 K), the “Turn” conformation had the lowest free energy, while, at higher temperatures (360 K), “E1” lies at the lowest free energy minimum. Free energies of the minima (in kJ/mol) and barriers between them are shown.

Thus, the stable conformation of the peptide switches from turn to extended conformation as the temperature rises. Also, upon a rise in temperature, the energy barrier between the turn and extended conformational ensembles decreases (Figure 12 and Figure S10 of the Supporting Information), thereby making the switching between two conformational states easier. The relatively faster switching of conformations between the two conformations was evident in DSSP plots also (Figure 3).

3.7. Turn Stabilizing Hydrogen Bonds and Y–Q Side-Chain Packing Interaction Are Associated with the “Turn” Minimum in the Free Energy Landscape. As discussed earlier, turn formation in YKGQ was facilitated by hydrogen bonds (QSNH:Y2CO and Y2NH:Q5OE1) and Y–Q

association. We constructed the probability contour plots for the frames possessing the two hydrogen bonds (Figure 13a)

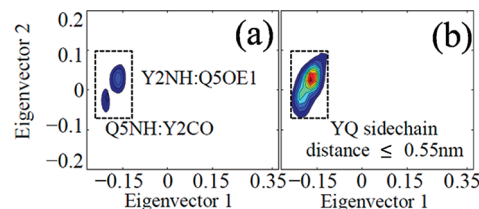


Figure 13. Probability contour plots for frames possessing (a) QSNH:Y2CO and Y2NH:Q5OE1 hydrogen bonds and (b) Y–Q side chain atoms distance ≤ 0.55 nm in the entire trajectory at 280 K, mapped on the essential plane, showing correspondence between the definition of turn ensemble (end-to-end distance <0.7 nm) followed by us in our thermodynamic analysis and the observed “Turn” minimum in the free energy landscape at 280 K (see Figure 3). Relatively higher frequency contours are represented by red color, while lower frequency contours are represented by blue color. In (b), lower contour levels (not visible in the figure) were observed to show a small population of Y–Q side-chain association for the extended conformations (see Figure 7 also).

and Y–Q side-chain association (Y–Q side chain atoms distance ≤ 0.55 nm, Figure 13b) in the essential plane, for 280 K simulation. These two parameters were also found to be associated with the “Turn” minimum observed in the essential plane (compare with Figure 2a). It may be noted that the contours for the two hydrogen bonds did not overlap, covering two different areas over the “Turn” minimum. This correlates with the observed exclusive existence of the two hydrogen bonds in the turn ensemble. Similar results were observed at all the other temperatures.

4. DISCUSSION

4.1. Intrapptide Interactions Dominate the Enthalpy of Turn Formation in YKGQ.

The enthalpy of turn formation

$(\Delta H_{U \rightarrow F})$, in YKGQ, may be considered to be comprised of intrapeptide interactions, like hydrogen bonds and side-chain association, peptide–water and water–water interactions. Our study indicates that intrapeptide interactions stabilize turn conformations, while solvent stabilizes unfolded conformations, at a given temperature. This is explained in what follows. Two significant hydrogen bonds—Q5NH:Y2CO and Y2NH:Q5OE1—were observed to drive the turn formation in YKGQ. These hydrogen bonds interchangeably switch their role in stabilizing the turn conformation, by forming only one bond at a time exclusively (section 3.3). As a result, one hydrogen bond is formed upon turn formation for a significant fraction of time at all temperatures. The observed change in folding enthalpy ($\Delta H_{U \rightarrow F}$) for turn formation at almost all temperatures (except 360–380 K) varies in the range of −8.1 kJ/mol at 280 K to −0.3 kJ/mol at 350 K (Figure 4 and Table S1 of the Supporting Information). The observed enthalpy change at lower temperatures is comparable to the strength of a single hydrogen bond. Moreover, it was observed that Y–Q side-chain packing interactions also stabilize the turn conformation (section 3.4). The percentage of hydrogen bond formation (Q5NH:Y2CO and Y2NH:Q5OE1, Figure 5) and Y–Q side-chain association (Figure 7) decreases with an increase in temperature, leading to increased $\Delta H_{U \rightarrow F}$ with a rise in temperature.

On examining the peptide–water and water–water hydrogen bonding propensities at various temperatures, it was observed that the unfolded conformations are relatively better stabilized by formation of a greater number (by one or two) of hydrogen bonds with water in comparison to the turn conformation, at all temperatures (Figure S11a of the Supporting Information). We note that almost no change in the number of water–water hydrogen bonds was observed, in the two conformational states, at a given temperature (Figure S11b of the Supporting Information). Since $\Delta H_{U \rightarrow F}$ increases with temperature (Figure 4), it can be inferred that intrapeptide interactions dominate $\Delta H_{U \rightarrow F}$ over peptide–water interactions.

4.2. Peptide Conformational Entropy Appears to Govern Temperature Dependence of the Entropy of Turn Formation. The entropy of turn formation ($\Delta S_{U \rightarrow F}$) can have contributions from the peptide conformational entropy and solvent entropy. For the turn ensemble, percentage sampling of Y–Q side-chain association was observed to decrease (Figure 7), indicating an increased degree of freedom for the two side-chains (Y2 and Q5) upon a rise in temperature. However, no significant change was observed in the case of the unfolded ensemble, for Y–Q association. Therefore, it may be anticipated that, with a rise in temperature, the entropy of the turn ensemble increases while the entropy of the unfolded ensemble essentially remains the same. This is also reflected by the increased broadening of Y–Q side-chain distance distribution plots (Figure 6 and Figure S7 of the Supporting Information) for the turn ensemble at high temperatures. Since broader distributions are associated with increased entropy, this observation suggests that the peptide conformational entropy of the turn increases with a rise in temperature. No significant broadening, at higher temperatures, was observed in the case of unfolded ensembles. Thus, it may be interpreted that the peptide conformational entropy for turn conformations increases with temperature and therefore contributes to an increase of $\Delta S_{U \rightarrow F}$ with temperature.

Solvent can also play an important role in stabilizing folded conformations through its interactions with hydrophobic and

hydrophilic residues. In the case of hydrophobic residues, the hydrophobic association decreases the exposed solvent accessible surface area and increases the solvent entropy, whereas, for hydrophilic residues, the attractive peptide–solvent interactions result in lowering of solvent entropy in the unfolded state. This effect may promote the folded state.⁴⁵ Considering the contribution of solvent entropy to $\Delta S_{U \rightarrow F}$ for YKGQ—being mainly a hydrophilic peptide in nature—solvent entropy may stabilize the turn (folded) conformation more than the unfolded conformation. However, as the temperature increases, the ordering of solvent molecules around polar side-chains may be distorted, leading to an increase in solvent entropy for the unfolded ensemble (S_U) with temperature. An opposite effect due to attractive polar side-chain–solvent interactions can be suspected for the turn conformational ensemble. With the increase in temperature, due to a decrease in Y–Q side-chain association, Y2 and Q5 side-chains in the turn conformation are relatively better solvent exposed. This is supported by the observed small increase in average SASA values for Y2 and Q5, for the turn ensemble, at higher temperatures (Figure 8 and Figure S8 of the Supporting Information). Due to the slightly improved side-chain–solvent interactions with temperature, the solvent molecules can be more ordered around the polar side-chains. This will induce a decrease in solvent entropy for the turn conformational ensemble (S_F) with an increase in temperature, though the effect can be small. Therefore, the increase in S_U and decrease in S_F , with a rise in temperature, would decrease the $\Delta S_{U \rightarrow F}$.

The two contributing factors—increased peptide conformational entropy and decreased solvent entropy—appear to oppose each other with a rise in temperature. Since the overall $\Delta S_{U \rightarrow F}$ for turn formation in YKGQ was observed to increase with a rise in temperature, it may be interpreted that it is the peptide conformational entropy that dominates the overall $\Delta S_{U \rightarrow F}$.

4.3. Comparison with Experimental Data. Capasso et al. examined the folding of a type II' β -turn forming aminosuccinyl peptide, Boc-L-Asu-Gly-L-Ala-OMe in a chloroform–acetonitrile mixture, using temperature dependent circular dichroism (CD) study.⁴⁶ This peptide has been reported to adopt a turn conformation in solvents with a weak hydrogen bond forming capacity.^{47,48} They observed $\Delta H_{U \rightarrow F}$ and $\Delta S_{U \rightarrow F}$ values of -6.6 ± 0.1 kJ mol^{−1} and -26.2 ± 0.6 J K^{−1} mol^{−1}, respectively, at 298 K for folding of the aminosuccinyl peptide. These values are very close to those observed for β -turn formation in YKGQ, with a $\Delta H_{U \rightarrow F}$ value of -6.0 kJ mol^{−1} and $\Delta S_{U \rightarrow F}$ value of -27.9 J K^{−1} mol^{−1} at 300 K. The β -turn stability of aminosuccinyl peptide was explained on the basis of intramolecular hydrogen bond formation between the urethane CO and alanine NH. The β -turn in YKGQ too was observed to be stabilized by formation of two intrapeptide hydrogen bonds—Q5NH:Y2CO and Y2NH:Q5OE1.

Temperature dependent NMR and CD analysis on a type VIII β -turn forming sequence GDNP suggested more folded conformations at lower temperatures,¹⁴ in corroboration with higher β -turn propensity observed for YKGQ at lower temperatures. Though the observed positive $\Delta G_{U \rightarrow F}$ value from the MD simulation of GDNP (varying between 8 and 10.5 kJ mol^{−1}) as well as that of the YKGQ (varying between 1.5 and 3.5 kJ mol^{−1}) indicates a more favored extended conformation, a relatively smaller positive value indicates greater β -turn sampling in the case of YKGQ. For GDNP,

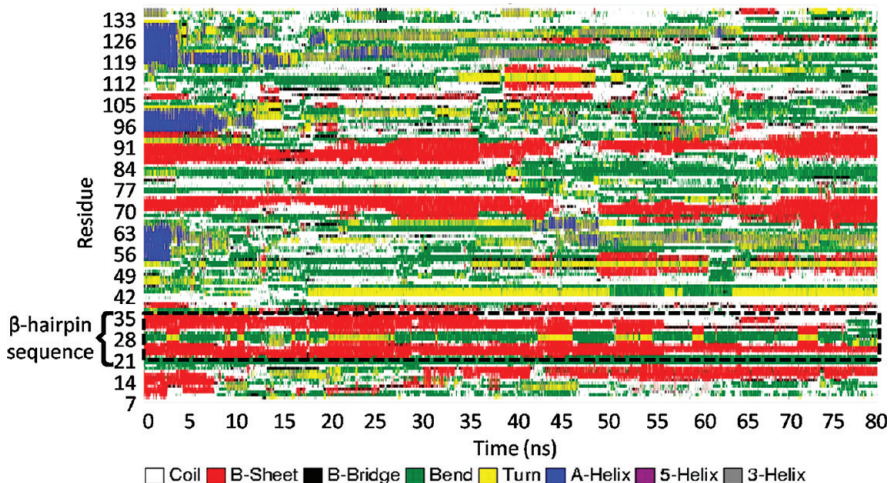


Figure 14. Variation of various secondary structures present in staphylococcal nuclease protein as a function of time, determined by the DSSP program,²⁷ at 500 K.

Fuchs et al. observed a $\Delta H_{U \rightarrow F}$ and $\Delta S_{U \rightarrow F}$ value of $-0.061 \text{ kJ mol}^{-1}$ and $-29.5 \text{ J K}^{-1} \text{ mol}^{-1}$.

Dyson et al. examined the turn propensities in a series of variants of the peptide sequence YPXDV and YPYXV, from influenza virus hemagglutinin, in water by ^1H NMR.⁴⁹ They observed a high β -turn propensity of $\sim 50\%$ for the *trans* form of the sequence YPGDV at 293 K, in water. Similarly, in our study, YKGQ displayed a high β -turn propensity at lower temperatures, being $\sim 34\%$ at 280 K, whereas $\sim 70\%$ of the *cis* isomer of AYPYDV and SYPYDV was observed to fold into a type VI β -turn at 278 K.⁴⁹ However, another NMR study on the *cis* isomer of SYPFDV, by Yao et al., revealed that a peptide sequence with a *cis*-Pro flanked by two aromatic residues and charged groups at N and C terminals further enhances the turn propensity.⁵⁰ These studies further reinforce the observation that even short peptide sequences can adopt significant populations of folded conformations in water.

4.4. Removing a Proline Residue from the YKGQP Sequence Does Not Affect the Turn Propensity of YKGQ. As mentioned earlier, YKGQ is a peptide sequence that connects the two strands of a native β -hairpin ($^{21}\text{DTVKLMYKGQPMTFR}^{35}$) present in staphylococcal nuclease, and folding study of the hairpin sequence⁴ and smaller sequence⁵ YKGQP shows that a hydrophobic association between Y and P is important for initiating the formation of β -hairpin. Our study demonstrates that even in the absence of P (Y-P association) YKGQ folds to adopt a β -turn conformation, which could nucleate β -hairpin formation. Thus, it suggests that it is the basic turn propensity of the YKGQ sequence that drives the β -hairpin formation of $^{21}\text{DTVKLMYKGQPMTFR}^{35}$.

4.5. YKGQ Appears to Be an Active β -Turn. The turn conformation sampled by YKGQ could be an active β -turn. Numerous studies indicate the role played by turns in nucleating folding of secondary structures like β -sheets.^{39,51–54}

It has been suggested that protein folding initiated by turn formation demands modest loss in conformational entropy, as only local interactions are at play.⁵⁵ While some turns play an active role in folding by taking part in the folding process, some turns may remain passive elements of folding.^{6–8} Thus, it is important to investigate the energetics involved in formation of this important protein segment which governs the fate of the protein chain. Our study demonstrates that the short tetra-

peptide sequence YKGQ folds to adopt a β -turn conformation irrespective of its missing protein context, thus indicating an intrinsic propensity of the sequence to adopt a turn conformation. Therefore, we may infer, based on current results and earlier studies,^{4,5} that YKGQ is an active β -turn.

4.6. β -Turn Propensity in YKGQ Persists Even at Higher Temperatures: Implications for Protein Folding. Higher thermostability has been observed in the case of proteins from thermophilic organisms, under temperature extremes. Comparison of structural features of thermophilic proteins with their mesophilic counterparts seems to suggest that factors like higher number of salt-bridges, hydrogen bonds, and stable hydrophobic core lead to compact structures and are found to be responsible for greater thermostability of thermophilic proteins.^{56–59} Stable loops can also be a factor in increasing thermostability. Loop rigidification by proline residues has been suggested to be a contributing factor for thermal stability.⁶⁰ A chimeric protein, made of parts from a thermophilic protein form *Thermus thermophilus* and a mesophilic protein from *Bacillus subtilis*, was found to be less stable than the wild type thermophilic protein.⁶¹ Four single-site mutations in loop regions, of the mesophilic part by corresponding residues in the thermophilic protein, stabilized the chimeric protein significantly, indicating the role played by loop regions. A similar observation was made by Jang et al.⁶² when removal of a small loop segment from a thermostable protease, thermicin, lowered the unfolding temperature (T_m) by 14 °C than that for the parent thermicin. Studies like these point to the importance of loops in maintaining the thermostability of certain thermophilic proteins.

Therefore, our observation of persistent β -turn conformation in YKGQ even at higher temperatures (section 3.2) seems to hold significance for the role of thermostable turns in protein folding and stability of such proteins. For instance, a loop or turn that is stable even at higher temperatures may function as a protein folding initiator and contribute to protein stability through entropic advantage. The sequence YKGQP, as explained in the Introduction, is known to facilitate the formation of β -hairpin through both experiments^{2,3} and simulations.^{4,5} Since the sequence YKGQ forms a “thermostable turn”, it is of interest to examine if the β -hairpin nucleated by such a turn is also a stable structure with respect to temperature. Protein unfolding MD simulations at higher

temperatures can be used to infer the role played by various sequence regions of the protein in protein folding.^{63–66} We performed a 80 ns long MD simulation of the staphylococcal nuclease at an elevated temperature of 500 K to further investigate the structural stability of the β -hairpin as a part of nuclease protein. Our results revealed that the β -hairpin comprising the sequence YKGQ at the reverse turn was one of the last secondary structures to unfold, suggesting that this structure is relatively stable with respect to thermal stress (Figure 14).

Proteins can be stabilized by adding glycine residues at certain positions in β -turns.^{67–71} Since glycine can sample more conformational space in all four quadrants of the Ramachandran map, it decreases the steric strain in the folded protein conformations and also promotes turn conformations. In fact, it has been observed that glycine is the most frequently possessed amino acid by different types of turns.^{72–75} A large reduction observed in the turn propensity observed in the Gly4 \rightarrow Ala4 mutant of YKGQP also reflects the importance of glycine in promoting the turn formation in YKGQP.⁵ Therefore, the enhanced stability observed for the YKGQ turn at high temperatures could be originating from the presence of a glycine residue in the sequence of the turn.

5. CONCLUSIONS

The sequence YKGQ from staphylococcal nuclease has inherent turn propensity, even in the absence of the parent hairpin context. This has implications for the folding of β -hairpin from nuclease, which was shown to be an early folding event by both experiments and simulations. Our work has shown that the turn propensity at lower temperatures is favored by enthalpy, while turn propensity at higher temperatures is favored by entropy. Intrapptide interactions were observed to dominate the temperature dependence of enthalpy of turn formation, while the peptide (side-chain) conformational entropy dominates the entropy of turn formation. Two significant hydrogen bonds (Q5NH:Y2CO and Y2NH:Q5OE1) contribute to the stabilization of closed β -turns, while water bridges (forming intermolecular peptide–water hydrogen bonds) stabilize open β -turns. Association of Y and Q side-chains was also seen to contribute significantly to the turn propensity. The turn and extended conformational ensembles are separated by modest free energy barriers. Observation of turn conformations even at higher temperatures may have significance for folding of thermophilic proteins. The β -hairpin from staphylococcal nuclease with YKGQ at the turn region is found to be one of the last secondary structures to unfold during a thermal denaturation simulation of staphylococcal nuclease at 500 K, indicating its relative stability to thermal stress. These results highlight that thermodynamic study of turn and loop regions at higher temperatures might provide insights into the stability and folding of thermophilic proteins.

■ ASSOCIATED CONTENT

Supporting Information

In the text, we have presented the results mainly for a lower temperature simulation (at 280 K) and a higher temperature simulation (at 360 K). Results obtained at other temperatures have been presented in Figures S1–S11 and Table S1 of the Supporting Information. This material is available free of charge via the Internet at <http://pubs.acs.org>.

■ AUTHOR INFORMATION

Corresponding Author

*E-mail: sasidhar@chem.iitb.ac.in. Phone: +91-22-2576 7179. Fax: +91-22-2576 3480.

Notes

The authors declare no competing financial interest.

■ ACKNOWLEDGMENTS

We thank BRNS for funding the research through a research grant, sanction number 2007/37/32/BRNS/1909, sanctioned to Y.U.S., and H.K. thanks the CSIR for a Senior Research Fellowship (award no. 09/087 0529/2008-EMR-I).

■ REFERENCES

- (1) Loll, P. J.; Lattman, E. E. *Proteins* **1989**, *5*, 183–201.
- (2) Jacobs, M. D.; Fox, R. O. *Proc. Natl. Acad. Sci. U.S.A.* **1994**, *91*, 449–453.
- (3) Walkenhorst, W. F.; Edwards, J. A.; Markley, J. L.; Roder, H. *Protein Sci.* **2002**, *11*, 82–91.
- (4) Patel, S.; Sista, P.; Balaji, P. V.; Sasidhar, Y. U. *J. Mol. Graphics Modell.* **2006**, *25*, 103–115.
- (5) Patel, S.; Sasidhar, Y. U. *J. Pept. Sci.* **2007**, *13*, 679–692.
- (6) McCallister, E. L.; Alm, E.; Baker, D. *Nat. Struct. Biol.* **2000**, *7*, 669–673.
- (7) Chang, S.-G.; Choi, K.-D.; Kim, D.-Y.; Kang, H.-T.; Song, M.-C.; Shin, H.-C. *Bull. Korean Chem. Soc.* **2002**, *23*, 1369–1370.
- (8) Marcelino, A. M. C.; Giersch, L. M. *Biopolymers* **2008**, *89*, 380–391.
- (9) Daura, X.; van Gunsteren, W. F.; Mark, A. E. *Proteins* **1999**, *34*, 269–280.
- (10) Daidone, I.; Amadei, A.; Di Nola, A. *Proteins* **2005**, *59*, 510–518.
- (11) Boned, R.; van Gunsteren, W. F.; Daura, X. *Chem.—Eur. J.* **2008**, *14*, 5039–5046.
- (12) Yang, L.; Shao, Q.; Gao, Y. Q. *J. Phys. Chem. B* **2009**, *113*, 803–808.
- (13) Demchuk, E.; Bashford, D.; Gippert, G. P.; Case, D. A. *J. Mol. Biol.* **1997**, *270*, 305–317.
- (14) Fuchs, P. F.; Bonvin, A. M.; Bochicchio, B.; Pepe, A.; Alix, A. J.; Tamburro, A. M. *Biophys. J.* **2006**, *90*, 2745–2759.
- (15) Woutersen, S.; Hamm, P. *J. Chem. Phys.* **2001**, *114*, 2727–2737.
- (16) Eker, F.; Cao, X.; Nafie, L.; Schweitzer-Stenner, R. *J. Am. Chem. Soc.* **2002**, *124*, 14330–14341.
- (17) Shi, Z.; Olson, C. A.; Rose, G. D.; Baldwin, R. L.; Kallenbach, N. R. *Proc. Natl. Acad. Sci. U.S.A.* **2002**, *99*, 9190–9195.
- (18) Kentsis, A.; Mezei, M.; Gindin, T.; Osman, R. *Proteins* **2004**, *55*, 493–501.
- (19) Mezei, M.; Fleming, P. J.; Srinivasan, R.; Rose, G. D. *Proteins* **2004**, *55*, 502–507.
- (20) Berendsen, H. J. C.; Postma, J. P. M.; van Gunsteren, W. F.; Hermans, J. In *Intermolecular Forces*; Pullmann, B., Ed.; D. Reidel Publishing Company: Dordrecht, The Netherlands, 1981; pp 331–342.
- (21) Hess, B.; Kutzner, C.; van der Spoel, D.; Lindahl, E. *J. Chem. Theory Comput.* **2008**, *4*, 435–447.
- (22) Jorgensen, W. L.; Tirado-Rives, J. *J. Am. Chem. Soc.* **1988**, *110*, 1657–1666.
- (23) Darden, T.; York, D.; Pedersen, L. *J. Chem. Phys.* **1993**, *98*, 10089–10092.
- (24) Essmann, U.; Perera, L.; Berkowitz, M.; Darden, T.; Lee, H.; Pedersen, L. *J. Chem. Phys.* **1995**, *103*, 8577–8593.
- (25) Hess, B.; Bekker, H.; Berendsen, H. J. C.; Fraaije, J. G. E. M. *J. Comput. Chem.* **1997**, *18*, 1463–1472.
- (26) Berendsen, H. J. C.; Postma, J.; DiNola, A.; Haak, J. *J. Chem. Phys.* **1984**, *81*, 3684–3690.
- (27) Kabsch, W.; Sander, C. *Biopolymers* **1983**, *22*, 2577–2637.

- (28) Daura, X.; Gademann, K.; Jaun, B.; Seebach, D.; van Gunsteren, W. F.; Mark, A. E. *Angew. Chem., Int. Ed.* **1999**, *38*, 236–240.
- (29) Humphrey, W.; Dalke, A.; Schulten, K. *J. Mol. Graphics* **1996**, *14*, 33–38.
- (30) Lewis, P. N.; Momany, F. A.; Scheraga, H. A. *Biochim. Biophys. Acta* **1973**, *303*, 211–229.
- (31) Venkatachalam, C. M. *Biopolymers* **1968**, *6*, 1425–1436.
- (32) Crawford, J. L.; Lipscomb, W. N.; Schellman, C. G. *Proc. Natl. Acad. Sci. U.S.A.* **1973**, *70*, 538–542.
- (33) Lewis, P. N.; Momany, F. A.; Scheraga, H. A. *Proc. Natl. Acad. Sci. U.S.A.* **1971**, *68*, 2293–2297.
- (34) Chou, P. Y.; Fasman, G. D. *Biochemistry* **1974**, *13*, 222–245.
- (35) Richardson, J. S. *Adv. Protein Chem.* **1981**, *34*, 167–339.
- (36) Wilmot, C. M.; Thornton, J. M. *J. Mol. Biol.* **1988**, *203*, 221–232.
- (37) Amadei, A.; Linssen, A. B.; Berendsen, H. J. C. *Proteins* **1993**, *17*, 412–425.
- (38) de Groot, B. L.; Amadei, A.; Scheek, R. M.; van Nuland, N. A.; Berendsen, H. J. C. *Proteins* **1996**, *26*, 314–322.
- (39) Thukral, L.; Smith, J. C.; Daidone, I. *J. Am. Chem. Soc.* **2009**, *131*, 18147–18152.
- (40) Pettitt, B. M.; Karplus, M. *Chem. Phys. Lett.* **1987**, *136*, 383–386.
- (41) van der Spoel, D.; van Buuren, A. R.; Tieleman, D. P.; Berendsen, H. J. C. *J. Biomol. NMR* **1996**, *8*, 229–238.
- (42) Durate, A. M. S.; van Mierlo, C. P. M.; Hemminga, M. A. *J. Phys. Chem. B* **2008**, *112*, 8664–8671.
- (43) Karvounis, G.; Nerukh, D.; Glen, R. C. *J. Chem. Phys.* **2004**, *121*, 4925–4934.
- (44) Patel, S.; Taimni, R.; Sasidhar, Y. U. *Protein Pept. Lett.* **2007**, *14*, 581–589.
- (45) Noé, F.; Daidone, I.; Simth, J. C.; Di Nola, A.; Amadei, A. *J. Phys. Chem. B* **2008**, *112*, 11155–11163.
- (46) Capasso, S.; Mazzarella, L.; Zagari, A. *Chirality* **1995**, *7*, 605–609.
- (47) Capasso, S.; Mattia, C. A.; Mazzarella, L.; Zagari, A. *Int. J. Pept. Protein Res.* **1984**, *24*, 85–95.
- (48) Capasso, S.; Mazzarella, L.; Sica, F.; Zagari, A. *Int. J. Pept. Protein Res.* **1984**, *24*, 588–596.
- (49) Dyson, H. J.; Rance, M.; Houghten, R. A.; Lerner, R. A.; Wright, P. E. *J. Mol. Biol.* **1988**, *201*, 161–200.
- (50) Yao, J.; Dyson, H. J.; Wright, P. E. *J. Mol. Biol.* **1994**, *243*, 754–766.
- (51) Jager, M.; Nguyen, H.; Crane, J. C.; Kelly, J. W.; Gruebele, M. *J. Mol. Biol.* **2001**, *311*, 373–393.
- (52) Jager, M.; Deechongkit, S.; Koepf, E. K.; Nguyen, H.; Gao, J.; Powers, E. T.; Gruebele, M.; Kelly, J. W. *Pept. Sci.* **2008**, *90*, 751–758.
- (53) Fuller, A. A.; Du, D.; Liu, F.; Davoren, J. E.; Bhabha, G.; Kroon, G.; Case, D. A.; Dyson, H. J.; Powers, E. T.; Wipf, P.; Gruebele, M.; Kelly, J. W. *Proc. Natl. Acad. Sci. U.S.A.* **2009**, *106*, 11067–11072.
- (54) Shao, Q.; Wei, H.; Gao, Y. Q. *J. Mol. Biol.* **2010**, *402*, 595–609.
- (55) Zimmerman, S. S.; Scheraga, H. A. *Proc. Natl. Acad. Sci. U.S.A.* **1977**, *74*, 4126–4129.
- (56) Kumar, S.; Nussinov, R. *Cell. Mol. Life Sci.* **2001**, *58*, 1216–1233.
- (57) Vieille, C.; Ziekus, G. *J. Microbiol. Mol. Biol. Rev.* **2001**, *65*, 1–43.
- (58) Razvi, A.; Scholtz, J. M. *Protein Sci.* **2006**, *15*, 1569–1578.
- (59) Barzegar, A.; Moosavi-Movahedi, A. A.; Pedersen, J. Z.; Miroliae, M. *Enzyme Microb. Technol.* **2009**, *45*, 73–79.
- (60) Matthews, B. W.; Nicholson, H.; Becktel, W. J. *Proc. Natl. Acad. Sci. U.S.A.* **1987**, *84*, 6663–6667.
- (61) Numata, K.; Hayashi-Iwasaki, Y.; Kawaguchi, J.; Sakurai, M.; Moriyama, H.; Tanaka, N.; Oshima, T. *Biochim. Biophys. Acta* **2001**, *1545*, 174–183.
- (62) Jang, H. J.; Lee, C.-H.; Lee, W.; Kim, Y. S. *J. Biochem. Mol. Biol.* **2002**, *35*, 498–507.
- (63) Day, R.; Daggett, V. *Adv. Protein Chem.* **2003**, *66*, 373–403.
- (64) Day, R.; Daggett, V. *J. Mol. Biol.* **2007**, *366*, 677–686.
- (65) McCully, M. E.; Beck, D. A. C.; Daggett, V. *Biochemistry* **2008**, *47*, 7079–7089.
- (66) Mehareenna, Y. T.; Poulos, T. L. *Biochemistry* **2010**, *49*, 6680–6686.
- (67) Kimura, S.; Kanaya, S.; Nakamura, H. *J. Biol. Chem.* **1992**, *267*, 22014–22017.
- (68) Stites, W. E.; Meeker, A. K.; Shortle, D. *J. Mol. Biol.* **1994**, *235*, 27–32.
- (69) Masumoto, K.; Ueda, T.; Motoshima, H.; Imoto, T. *Protein Eng., Des. Sel.* **2000**, *13*, 691–695.
- (70) Takano, K.; Yamagata, Y.; Yutani, K. *Proteins* **2001**, *45*, 274–280.
- (71) Fu, H.; Grimsley, G. R.; Razvi, A.; Scholtz, J. M.; Pace, C. N. *Proteins* **2009**, *77*, 491–498.
- (72) Sibanda, B. L.; Blundell, T. L.; Thornton, J. M. *J. Mol. Biol.* **1989**, *206*, 759–777.
- (73) Sibanda, B. L.; Thornton, J. M. *Methods Enzymol.* **1991**, *202*, 59–82.
- (74) Kwasigroch, J.-M.; Chomilier, J.; Mornon, J.-P. *J. Mol. Biol.* **1996**, *259*, 855–872.
- (75) Nagi, A. D.; Anderson, K. S.; Regan, L. *J. Mol. Biol.* **1999**, *286*, 257–265.